

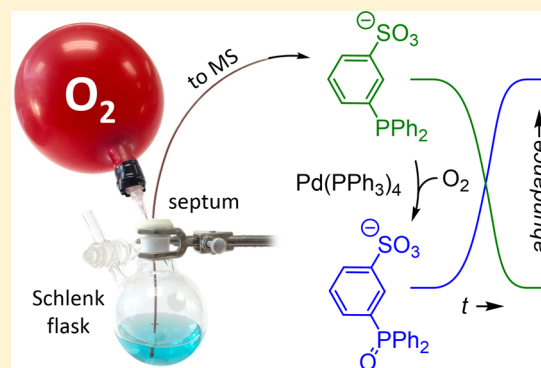
## Simplified Real-Time Mass Spectrometric Analysis of Reactions

Amelia V. Hesketh, Steven Nowicki, Kristen Baxter, Rhonda L. Stoddard, and J. Scott McIndoe\*

Department of Chemistry, University of Victoria, P.O. Box 3065 Victoria, BC V8W3 V6, Canada

## Supporting Information

**ABSTRACT:** Dynamic information can be obtained on in-progress reactions in real time using a balloon-pressurized Schlenk flask in combination with an electrospray ionization mass spectrometer. The apparatus can be set up on a Schlenk line or in a glovebox and transported to the spectrometer, to be initiated by addition of catalyst or reactant by syringe through a septum. The system is demonstrated on palladium-catalyzed oxidation of phosphines.



## INTRODUCTION

Electrospray ionization mass spectrometry (ESI-MS) is fast and sensitive,<sup>1</sup> can handle complex mixtures,<sup>2</sup> and has a wide dynamic range<sup>3</sup>—all properties that make it useful for analysis of chemical reactions. Performing such experiments continuously is a critical element, granting experimenters the dynamic information craved by chemists with a mechanistic bent. We recently published a method for moving a reacting solution from flask to mass spectrometer called “pressurized sample infusion” (PSI)<sup>4,5</sup> that has found use by others.<sup>6,7</sup> Essentially, it involves a cannula transfer from a Schlenk flask through  $\sim 100$   $\mu\text{m}$  inner diameter tubing, using an overpressure of 1–5 psi to generate a flow rate of  $\sim 10$   $\mu\text{L}\cdot\text{min}^{-1}$ . Here, we have simplified this setup still further by recognizing that a small overpressure of this magnitude is easily delivered by a party balloon. We developed this to improve accessibility and flexibility of PSI. It is now: (a) highly portable, and samples can be made up on a Schlenk line, the balloon attached, and the whole apparatus moved to the mass spectrometer while under a positive pressure; (b) easily relocatable, as addition of an inflator to a glovebox allows for PSI experiments to be conducted inside (presupposing the instrument is nearby);<sup>8</sup> (c) inexpensive, there being no requirement for a special regulator or an additional supply of pressurized gas located near the mass spectrometer; (d) versatile, as the balloon can be inflated with any gas, allowing experiments to be conducted under whatever atmosphere is required, and increased pressures can be achieved by using two (or even three) balloons, one inside the other, and multiple layers of balloon decrease the effectiveness of inward diffusion of atmospheric gases; and (e) safe, because accidental overpressurization is impossible, the balloon functioning as its own pressure relief valve.

Previously, the delivery of inert gases via balloon has been described for safe reactions by students<sup>9</sup> and researchers,<sup>10</sup> for

safe delivery of air-sensitive organometallic reagents,<sup>11,12</sup> and for oxidation reactions with  $\text{O}_2$  at 1 atm.<sup>13</sup>

## RESULTS AND DISCUSSION

**Balloon Pressure during Inflation.** Balloon pressure was experimentally quantified by attaching an air cylinder to a balloon equipped with a low range (0–15 psi) pressure gauge. The air source was set to a constant flow rate, and the pressure of the system was monitored until the balloon(s) burst. These data allowed the pressure of the balloon to be plotted as a function of volume of air delivered (Figure 1).

Initially, the pressure increased dramatically with relatively little volume added. Thereafter, the balloon began to inflate and

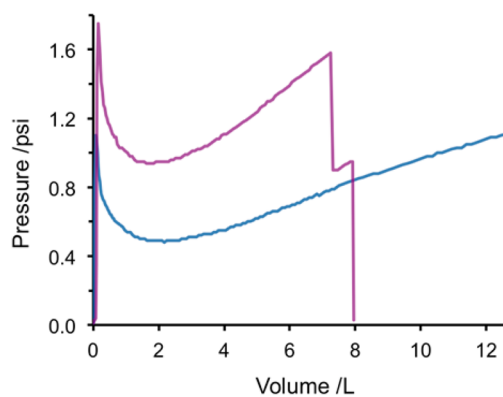


**Figure 1.** Dependence of balloon pressure on volume of air added during inflation for a single balloon (blue) and double balloon (purple).

Received: May 28, 2015

Published: July 23, 2015

a decrease in pressure was observed. A near linear pressure–volume relationship was observed for all balloons between 2 L inflation volume and maximum volume (bursting). Figure 1 highlights several important experimental considerations for applying balloon-driven PSI ESI-MS. Balloons are limited in the pressure they can impose on a closed system: a single balloon can provide  $\sim 1$  psi, while a double balloon can provide  $\sim 1.5$  psi. Over the operating volume ranges, balloon pressure changes relatively little (e.g., between 1 and 5 L, pressure ranges between 0.45 and 0.65 psi); therefore, reproducibility of experimentation can be achieved since deflation of the balloon results in little pressure variation. The reproducibility of the pressure/volume traces is very good, but in practice, this is only true between balloons of the same age and brand. The balloons used here were “helium-quality” party balloons.

**Flow Rate Monitoring.** ESI-MS requires that a solution enter a mass spectrometer with a constant flow rate to avoid irregularities in data. Thus, a constant positive pressure must be maintained in the reaction vessel of a PSI ESI-MS setup during analysis. The stability of balloon pressure over time was assessed to ascertain the suitability of a balloon as a pressure source for PSI ESI-MS. An inflated balloon was attached to a sealed Schlenk flask containing methanol. PEEK tubing of 0.005" (127  $\mu\text{m}$ ) or 0.007" (178  $\mu\text{m}$ ) inner diameter was submerged in the methanol and fed through a rubber septum to a tared flask on an analytical balance. The mass of methanol delivered was recorded every 2 min for 90 min to determine the flow rate of the system.

The results of one such experiment are shown in Figure 2. The pressure exerted by the double balloon dipped appreciably

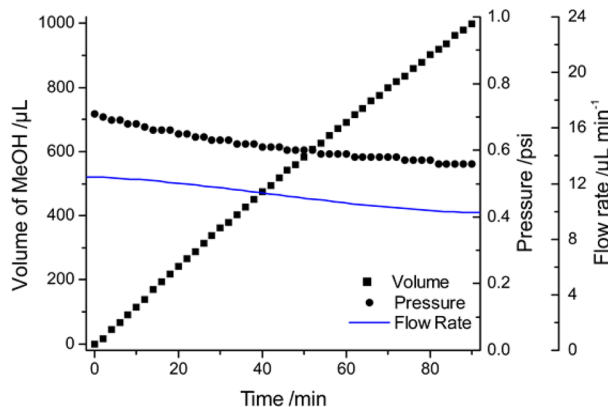


**Figure 2.** Volume of methanol delivered from a double-balloon pressurized Schlenk tube using 178  $\mu\text{m}$  ID PEEK tubing over time. Balloon pressure was also monitored. Differentiation of a polynomial best-fit line for the volume data was used to obtain flow rate.

over 90 min (from 0.71 to 0.56 psi), and this change had a proportional effect on the flow rate (as expected from the Hagen–Poiseuille equation). The natural stretching and deformation of the balloon’s latex walls in response to high pressure may account for the initially rapid and later gradual decline in pressure observed. However, ESI mass spectra are not especially sensitive to flow rate, and generally, we are more interested in relative changes than absolute ones (which is why PSI data are typically normalized to an internal standard or the total ion current).

To demonstrate the efficacy of this approach, we studied the catalytic oxidation of triphenylphosphine by dioxygen mediated by  $\text{Pd}(\text{PPh}_3)_4$ . We noticed that, in cases where  $\text{Pd}(\text{PPh}_3)_4$  is

added to the charged ligand  $[\text{PPN}][\text{PPh}_2(m\text{-C}_6\text{H}_4\text{SO}_3)]$  ( $[\text{PPN}][1]$ ) without the rigorous exclusion of oxygen, the palladium catalyst rapidly added dioxygen to form  $[\text{Pd}(\text{PPh}_3)(1)(\text{O}_2)]^-$  and catalyzed the formation of the phosphine oxide of **1** (**10**, Figure 3). The appearance of the phosphine oxide is a good indicator of a less-than-perfect air-free technique, though of course such conditions are typical of many catalytic reactions.

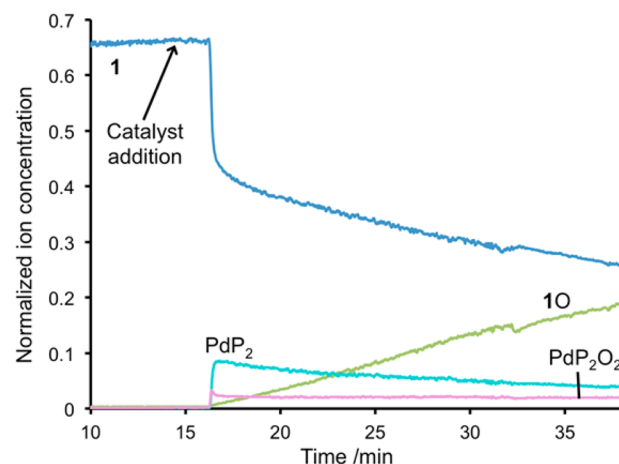


**Figure 3.** Addition of  $\sim 0.5 \text{ mmol L}^{-1}$   $\text{Pd}(\text{PPh}_3)_4$  to 2 equiv of  $[\text{PPN}][1]$  in dichloromethane in the presence of trace amounts of air.

**Catalytic Oxidation of  $[\text{PPN}][1]$ .** Phosphine oxides are often undesirable side products that form in catalytic reactions involving  $\text{PR}_3$  and late transition metals, such as Pt or Pd.<sup>14</sup> In 1977, Sen and Halpern detailed a mechanism for this reaction in which dioxygen forms an adduct with the 16-electron complex  $\text{Pt}^0(\text{PPh}_3)_3$  to generate  $\text{Pt}(\text{PPh}_3)_2\text{O}_2$  as an intermediate species while generating free  $\text{PPh}_3$  *in situ*. As determined by  $^{31}\text{P}$  NMR and cyclic voltammetry, they deduced that the oxygen does not directly transfer to the phosphine, but instead, the nucleophilic triphenylphosphine attacks the metal–oxygen complex, displacing and leaving with the oxygen.<sup>15</sup> They found that displacement of the oxygen was rate-limiting. In order to elucidate a mechanism, they required the use of more reactive phosphines to speed up the rate-limiting step relative to the later faster steps, and to enable detection of the  $\text{Pt}(\text{PPh}_3)_2\text{O}_2$  species.

Oxidation of  $\text{PPh}_3$  to  $\text{OPPh}_3$  has been previously reported using  $\text{Pt}^{0,16,17}$  and  $\text{Pd}^0$  catalysts.<sup>18,19</sup> Catalysis involving  $\text{Pd}^{\text{II}}$  has also shown reduction to  $\text{Pd}^0$  in conjunction with the oxidation of phosphines; in numerous examples, many involving palladium acetate,<sup>20–22</sup> the divalent Pd catalyst is reduced to  $\text{Pd}^{0,23}$  or other  $\text{Pd}^{\text{II}}$  catalysts.<sup>24</sup>  $\text{Pd}(\text{PPh}_3)_2\text{O}_2$  was isolated by Nyman, Wymore, and Wilkinson.<sup>25</sup> We set out to study the production of phosphine oxide with a  $\text{Pd}^0$  catalyst, planning to determine the rate of production of the oxide in pure oxygen as well as air. Deliberate addition of oxygen using an air- or oxygen-filled balloon as the PSI propellant allowed facile examination of this reaction under catalytic conditions. We tested three different sets of conditions: using an air-filled balloon and running the reaction with and without stirring, and using an oxygen-filled balloon with stirring (Figure 4). Note the similarity in the traces, suggesting that the reaction is insensitive to  $\text{O}_2$  concentration.

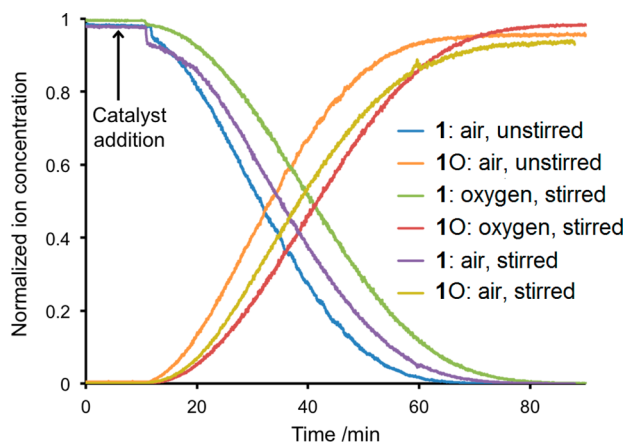


**Figure 4.** Catalytic oxidation of  $\sim 1 \text{ mmol L}^{-1}$  **1** under varying conditions with a  $\text{Pd}(\text{PPh}_3)_4$  catalyst loading of 20% monitored by single-balloon PSI ESI-MS (178  $\mu\text{m}$  ID PEEK tubing). Catalyst was added at 10 min and balloon pressure varied from 0.20 to 0.31 psi.

The kinetics of the reaction appear to be close to zero order ( $k = 0.27 \pm 0.02 \mu\text{mol}\cdot\text{s}^{-1}$  at the 95% confidence level) with an induction period before the maximum rate is obtained that varies slightly from one experiment to the next. The behavior of the palladium-containing species can also be inspected (Figure 5).

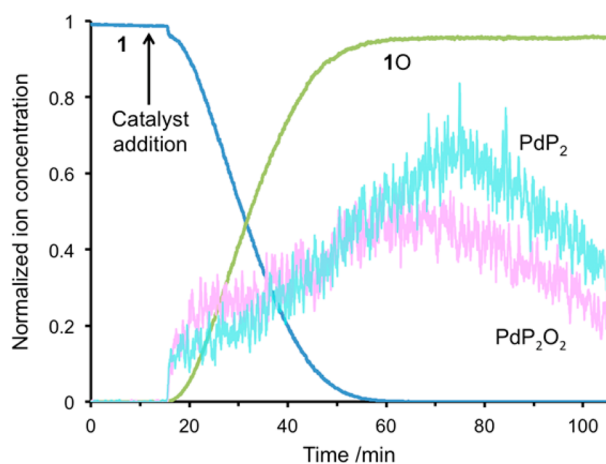


**Figure 5.** Oxidation of  $\sim 1 \text{ mmol L}^{-1}$  **1** in air with 40%  $\text{Pd}(\text{PPh}_3)_4$  catalyst loading monitored by single-balloon PSI ESI-MS with 177.8  $\mu\text{m}$  PEEK tubing (pressure = 0.25–0.31 psi) and moderate stirring. Catalyst was added at 15 min. Overlaid intermediates were scaled by 250 $\times$ .  $[\text{Pd}(\text{PPh}_3)(\mathbf{1})]^-$  and  $[\text{Pd}(\mathbf{1})_2]^{2-}$  were combined together to generate the trace labeled  $\text{PdP}_2$ , and analogous treatment was carried out for  $\text{PdP}_2(\text{O}_2)$ .

It is clear that exchange between  $\text{PPh}_3$  and **1** is fast and that the  $\text{PdP}_2(\text{O}_2)$  complex formed rapidly. The observed induction period is most likely a function of the  $\text{PPh}_3$  being oxidized preferentially before **1**. The abundance of the Pd-containing compounds does not seem to change much over the course of the reaction, and the  $\text{PdP}_2$  and  $\text{PdP}_2(\text{O}_2)$  complexes only disappear slowly once the reaction is over. The reaction does slow considerably as the phosphine is depleted, and the slow disappearance of the Pd-containing complexes at the conclusion of the reaction strongly implicates free phosphine in the reaction. However, we were curious as to how the reaction proceeded in the absence of free phosphine and

wondered whether another (slower) mechanism was operative. An MS/MS experiment was performed on  $[\text{Pd}(\text{PPh}_3)(\mathbf{1})(\text{O}_2)]^-$  wherein the complex was isolated and energized in the collision cell of the tandem mass spectrometer by accelerating the ions into (effectively) stationary argon atoms. The resulting fragments provide interesting information on the most energetically accessible decomposition pathways. Typically, transition-metal complexes decompose by loss of L-type donor ligands in collision-induced dissociation (CID),<sup>26</sup> but in some cases, more interesting processes can be observed. For example, palladium complexes may reductively eliminate a carbon–carbon bond in preference to simple phosphine ligand dissociation,<sup>27</sup> and this transformation is representative of its solution chemistry. In the case of  $[\text{Pd}(\text{PPh}_3)(\mathbf{1})(\text{O}_2)]^-$ , the MS/MS spectrum is at first glance unsurprising—the principal pathway of fragmentation is  $\text{O}_2$  loss (Figure 6).

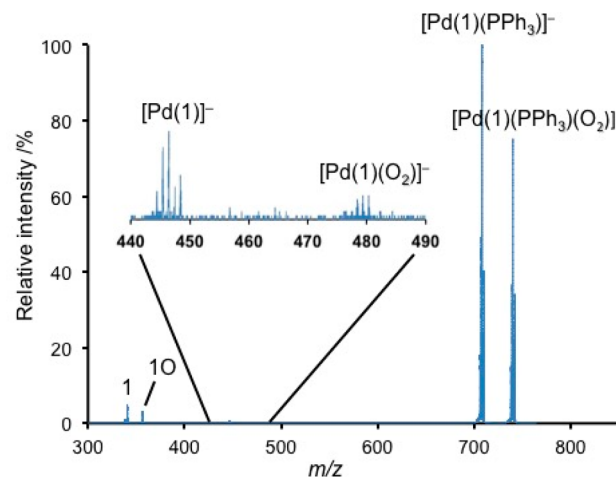
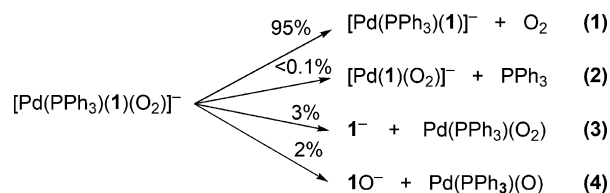


**Figure 6.** MS/MS of the key  $\text{Pd}(0)$  intermediate at  $m/z$  741.

However, close inspection of the lower mass region reveals that phosphine dissociation is competitive with phosphine oxide dissociation, suggesting that reaction 4 is an accessible gas-phase pathway for unimolecular decomposition (Scheme 1).

#### Scheme 1. Gas-Phase Decomposition of $[\text{Pd}(\text{PPh}_3)(\mathbf{1})(\text{O}_2)]^-$



Loss of  $\text{O}_2$ , **1**, and  $\text{PPh}_3$  can all be reasonably expected to be reversible in solution, so that leaves (4) as a low probability transformation but one that is unlikely to be reversible. Given that it happens in the gas phase, we assume it proceeds by some sort of concerted intramolecular process. The gas phase makes it impossible to observe a concerted intermolecular reaction between  $\text{L}_2\text{PdO}_2$  and P to generate  $\text{LPd}(\text{OP})_2$  as described by Chul and co-workers,<sup>23</sup> but the MS/MS data are sufficiently interesting that future attempts to computationally model this reaction should perhaps consider the possibility of such a unimolecular decomposition contributing to the overall reaction, and even dominating in the case of no free phosphine.

## EXPERIMENTAL SECTION

**Flow Rate Monitoring.** An Erlenmeyer flask was tared on an analytical balance. A 0.5 m length of PEEK tubing was clamped above the bottom of the flask and connected to a sealed Schlenk flask containing methanol through a rubber septum. The balloon(s) used were connected to the Schlenk flask via rubber tubing, and a T-piece was used to accommodate the attachment of a digital pressure gauge (Omega DPG1000B-15A).

**PSI ESI-MS Monitoring of [PPN][1] Oxidation.** [PPN][1] was made by previously established literature methods.<sup>27,28</sup> Solvents were HPLC grade and were purified on an MBraun solvent purification system and degassed before use. Glassware was oven-dried overnight before use. Reagents were stored and manipulated in a glovebox under an inert atmosphere. All mass spectra were collected on a Micromass Q-ToF Micro mass spectrometer in negative mode, using electrospray ionization: capillary voltage, 2900 V; extraction voltage, 1.5 V; source temperature, 65 °C; desolvation temperature, 165 °C; cone gas flow, 100 L/h; desolvation gas flow, 200 L/h; collision voltage, 2 V for MS experiments and 2–25 V for MS/MS experiments; MCP voltage, 2400 V. [PPN][1] (0.0100 g, 11.2 μmol) was dissolved in methanol (7 mL) in a Schlenk flask under N<sub>2</sub>. The flask was attached to a balloon and a pressure gauge with rubber tubing and a T-piece. The balloon was filled with the gas of choice (air, N<sub>2</sub>, or O<sub>2</sub>) and used to purge the flask, and then refilled with the correct gas prior to analysis. 178 μm ID PEEK tubing was immersed in the phosphine solution, and the other end of the tubing was connected to the MS source. Pd(PPh<sub>3</sub>)<sub>4</sub> (0.0026 g, 2.2 μmol for 20% loading or 0.0052 g, 4.5 μmol for 40% loading) was suspended in methanol (3 mL) and added by syringe to the stirring phosphine solution. The reaction was stopped when **1** had been completely or nearly completely replaced by **10**. Mass spectrometric interpretation was aided by ChemCalc online tools.<sup>29</sup>

Normalized ion concentration was established by dividing the intensity of the complete isotope pattern of a given species to the total ion current for each spectrum. No further manipulation or smoothing of the data was performed.

## ASSOCIATED CONTENT

### Supporting Information

Figures giving flow rate monitoring data for different initial pressure and PEEK tubing diameter conditions. The Supporting Information is available free of charge on the ACS Publications website at DOI: 10.1021/acs.organomet.5b00460.

## AUTHOR INFORMATION

### Corresponding Author

\*E-mail: mcindoe@uvic.ca (J.S.M.).

### Notes

The authors declare no competing financial interests.

## ACKNOWLEDGMENTS

J.S.M. thanks the Natural Sciences and Engineering Research Council (NSERC) of Canada, the Canada Foundation for Innovation (CFI), the British Columbia Knowledge Development Fund (BCKDF), and the University of Victoria for instrumentation and operational funding.

## REFERENCES

- (1) Bruins, A. P. *J. Chromatogr. A* **1998**, *794*, 345–357.
- (2) Fenn, J. B.; Mann, M.; Meng, C. K.; Wong, S. F.; Whitehouse, C. M. *Science* **1989**, *246*, 64–71.
- (3) Price, W. D.; Schnier, P. D.; Williams, E. R. *Anal. Chem.* **1996**, *68*, 859–866.
- (4) Vikse, K. L.; Ahmadi, Z.; Luo, J. W.; van der Wal, N.; Daze, K.; Taylor, N.; McIndoe, J. S. *Int. J. Mass Spectrom.* **2012**, *323–324*, 8–13.
- (5) Vikse, K. L.; Woods, M. P.; McIndoe, J. S. *Organometallics* **2010**, *29*, 6615–6618.

- (6) Gellrich, U.; Meißner, A.; Steffani, A.; Kähny, M.; Drexler, H.; Heller, D.; Plattner, D. A.; Breit, B. *J. Am. Chem. Soc.* **2013**, *136*, 1097–1104.
- (7) Lichtenthaler, M. R.; Higelin, A.; Kraft, A.; Hughes, S.; Steffani, A.; Plattner, D. A.; Slattery, J. M.; Krossing, I. *Organometallics* **2013**, *32*, 6725–6735.
- (8) Lubben, A. T.; McIndoe, J. S.; Weller, A. S. *Organometallics* **2008**, *27*, 3303–3306.
- (9) Bohac, A. *J. Chem. Educ.* **1995**, *72*, 263.
- (10) Cornell, C. N.; Sigman, M. S. *Org. Lett.* **2006**, *8*, 4117–4120.
- (11) Newton, T. A. *J. Chem. Educ.* **2005**, *82*, 936.
- (12) Pavia, D. L.; Lampman, G. M.; Kriz, G. S.; Engel, R. G. *A Microscale Approach to Organic Laboratory Techniques*, 3rd ed.; Finch, M., Ed.; Brooks/Cole: Belmont, CA, 2013.
- (13) Ye, X.; Johnson, M. D.; Diao, T.; Yates, M. H.; Stahl, S. S. *Green Chem.* **2010**, *12*, 1180–1186.
- (14) Gubelmann, M. H.; Williams, A. F. *Struct. Bonding (Berlin, Ger.)* **1984**, *55*, 1–65.
- (15) Sen, A.; Halpern, J. *J. Am. Chem. Soc.* **1977**, *99*, 8337–8339.
- (16) Birk, J. P.; Halpern, J.; Pickard, A. L. *J. Am. Chem. Soc.* **1968**, *90*, 4491–4492.
- (17) Halpern, J.; Pickard, A. L. *Inorg. Chem.* **1970**, *9*, 2798–2800.
- (18) Takahashi, S.; Kuroyama, Y. *J. Chem. Soc. Japan* **1966**, *87*, 610.
- (19) Wilke, G.; Schott, H.; Heimbach, P. *Angew. Chem.* **1967**, *79*, 62.
- (20) Grushin, V. V. *J. Am. Chem. Soc.* **1999**, *121*, 5831–5832.
- (21) Hayashi, S.; Hirano, K.; Yorimitsu, H.; Oshima, K. *J. Am. Chem. Soc.* **2007**, *129*, 12650–12651.
- (22) Ozawa, F.; Kubo, A.; Hayashi, T. *Chem. Lett.* **1992**, *21*, 2177–2180.
- (23) Chul, W. L.; Jae, S. L.; Nag, S. C.; Kye, D. K.; Sang, M. L.; Jae, S. O. *J. Mol. Catal.* **1993**, *80*, 31–41.
- (24) Grushin, V. V.; Alper, H. *Organometallics* **1993**, *12*, 1890–1901.
- (25) Nyman, C. J.; Wymore, C. E.; Wilkinson, G. *J. Chem. Soc. A* **1968**, *3*, 561–563.
- (26) Pike, S. D.; Pernik, I.; Theron, R.; McIndoe, J. S.; Weller, A. S. *J. Organomet. Chem.* **2015**, *784*, 75–83.
- (27) Vikse, K. L.; Henderson, M. A.; Oliver, A. G.; McIndoe, J. S. *Chem. Commun.* **2010**, *46*, 7412–7414.
- (28) Barton, M. R.; Zhang, Y.; Awood, J. D. *J. Coord. Chem.* **2002**, *55*, 969.
- (29) Patiny, L.; Borel, A. *J. Chem. Inf. Model.* **2013**, *53*, 1223–1228.